AGU ADVANCING EARTH AND SPACE SCIENCE

Geophysical Research Letters

RESEARCH LETTER
10.1029/2021GL093534

Key Points:

- The temperature evolution of the winter season Yellow Sea Warm Current was reconstructed over the past 8.8 kyr
- Abrupt multi-centennial to millennial scale changes are superimposed on a gradual cooling trend starting from ~5 ka to the present
- Western Pacific Warm Pool subsurface water cooling signal was transmitted by the Kuroshio Current into the southern Yellow Sea

Supporting Information:

Supporting Information may be found in the online version of this article.

Correspondence to:

D.-W. Li and M. Zhao,
ldw@ouc.edu.cn;
maxzhao@ouc.edu.cn

Citation:

Li, D.-W., Yu, M., Jia, Y., Steinke, S., Li, L., Xiang, R., & Zhao, M. (2021). Gradually cooling of the Yellow Sea Warm Current driven by tropical Pacific subsurface water temperature changes over the past 5 kyr. *Geophysical Research Letters*, *48*, e2021GL093534. https://doi.org/10.1029/2021GL093534

Received 23 MAR 2021
Accepted 5 MAY 2021

Gradually Cooling of the Yellow Sea Warm Current Driven by Tropical Pacific Subsurface Water Temperature Changes Over the Past 5 kyr

Da-Wei Li[1,2], Meng Yu[1,2], Yonghao Jia[1], Stephan Steinke[3], Li Li[1,2], Rong Xiang[4], and Meixun Zhao[1,2]

[1]Frontiers Science Center for Deep Ocean Multispheres and Earth System, and Key Laboratory of Marine Chemistry Theory and Technology, Ministry of Education, Ocean University of China, Qingdao, China, [2]Laboratory for Marine Ecology and Environmental Science, Qingdao National Laboratory for Marine Science and Technology, Qingdao, China, [3]Department of Geological Oceanography & State Key Laboratory of Marine Environmental Science (MEL), Xiamen University, Xiamen, China, [4]Key Laboratory of Ocean and Marginal Sea Geology, South China Sea Institute of Oceanology, Chinese Academy of Sciences, Guangzhou, China

Abstract The integrated effects of ocean-atmosphere dynamics on the temperature evolution in the western North Pacific marginal seas have remained elusive. In order to study mechanisms controlling southern Yellow Sea (YS) temperature changes, bottom water temperature (BWT) changes were reconstructed for the last 8.8 kyr by using the TEX^{L}_{86} index, which archives temperature signal of the winter season Yellow Sea Warm Current. Our results reveal a series of abrupt multi-centennial to millennial scale BWT changes (~1°C), superimposed on a gradual long-term cooling (>3°C) trend starting from ~5 ka to the present. The YS BWT changes are positively correlated with subsurface water temperature changes in the Western Pacific Warm Pool (WPWP). The Western Pacific Warm Pool subsurface water cooling signal was most likely transmitted by the Kuroshio Current into the southern YS, highlighting the role of WPWP in influencing thermodynamics of the extratropical regions during the Holocene.

Plain Language Summary The Yellow Sea (YS) is a semi-closed marginal sea located in the northwestern Pacific Ocean. During the winter season, the Yellow Sea Warm Current (YSWC) is driven by northwesterly winds, flowing into the southern YS along the west flank of the central trough. The YSWC, a continuation of the Kuroshio Current, brings warm equatorial Pacific water into the YS, leading to milder winters in the surrounding coastal cities compared with other cities on the same latitude in China. The YSWC is sensitive to changes in ocean-atmosphere dynamics. However, its evolution during the Holocene is not well understood. We reconstruct the winter season temperature changes of the YSWC during the last 8.8 kyr. We found warm temperatures during the mid-Holocene (8.8-5 ka) and a gradual cooling trend over the last 5 kyr, which coincides with subsurface water temperature changes in the Western Pacific Warm Pool (WPWP). We suggest that the tropical subsurface water temperature changes of the WPWP are most likely transmitted via the Kuroshio Current into the YS. Our results shed new light on our understanding of the role played by the WPWP water masses in regulating subtropical ocean dynamics and climate during the mid-to-late Holocene.

1. Introduction

The Western Pacific Warm Pool (WPWP) constitutes the warmest water masses and thus plays an important role in regulating earth's climate. Instrumental data reveal a gradual warming trend over the last 60 years in the WPWP (Solomon & Newman, 2012), the North Pacific western boundary currents, that is, the Kuroshio Current (Wu et al., 2012), and in the marginal seas of China (S. Park et al., 2011), most likely associated with the increase in greenhouse gas emissions. This motivates us to investigate low- to mid-latitude ocean thermodynamic teleconnection at both centennial- and millennial-time scales during the Holocene, which remains poorly understood. Numerous studies have demonstrated that the WPWP water heat content experienced a general scenario of an Early Holocene Thermal Maximum and a gradual decrease thereafter. The general Holocene decreasing trend in temperature is superimposed by multi-centennial-scale changes

(Linsley et al., 2010; Moffa-Sanchez et al., 2019; Rosenthal et al., 2013). However, the impact of the WPWP thermodynamic changes on the extratropical regions beyond the instrumental period is not well understood because Northern Hemisphere high-latitude oceans experienced similar Holocene temperature variations which could have been transferred to mid-latitude regions either by an atmospheric bridge or through the ocean "conveyor belt" (Sun et al., 2012; Wanner et al., 2011 and references therein).

The Yellow Sea (YS), a semiclosed shelf sea with an average water depth of ~44 m, is located in the northwestern Pacific Ocean. The climate and hydrography of the YS are primarily controlled by the seasonally reversing East Asian monsoon wind patterns and the northward intrusion of the Yellow Sea Warm Current (YSWC), a branch of the Kuroshio Current which transmits tropical ocean properties northward, during the boreal winter season. Hence, the YS provides an opportunity to investigate high- and low-latitude interactions of atmospheric and oceanic dynamics. Assuming that proxy-derived annual sea surface temperature (SST) evolution resembles that of winter season SSTs in the southern YS, previous studies have suggested that the millennial-scale evolution of SSTs in the YS is driven by changes in the intensity of the Kuroshio Current during the Holocene (Jia et al., 2019; Nan et al., 2017). On the other hand, centennial-scale SST changes in the YS are proposed to be driven by North Atlantic climate change through the top-down conveyor of East Asian Winter Monsoon (EAWM) (Jia et al., 2019; Nan et al., 2017; L. Wang et al., 2011) and/or as a direct response to changes in the Kuroshio Current intensity (Y. Zhang et al., 2019). However, little is known about the temperature variations of the winter season YSWC due to the scarcity of robust proxy records, limiting our understanding on mechanisms controlling southern YS temperature changes.

Here, we show a YSWC temperature record using an archeal membrane lipid-based paleothermometer, that is, the TEX^{L}_{86} index, from gravity core A03-B recovered from the southern YS (123°38′E, 35°28′N; core length: 301 cm, water depth 77.6 m). Given the maximum occurrence of marine Thaumarchaeota in the bottom of the southern YS, the TEX^{L}_{86} index is interpreted as a robust bottom water temperature (BWT) proxy (Xing et al., 2015; also see discussion in supporting information). Core A03-B is located in the center of the modern southern Yellow Sea Cold Water Mass (see Figure S1), which experiences no seasonal changes in temperature (S. Park et al., 2011). The southern Yellow Sea Cold Water Mass is a remnant of the YSWC water mass of the previous winter (S. Park et al., 2011), and therefore we consider the TEX^{L}_{86} derived BWT at site A03-B as a proxy for winter season YSWC temperatures. High sediment accumulation rate (~34 cm per thousand years) at the core location (Jia et al., 2019) allows the study of centennial-scale temperature variations.

2. Materials and Methods

2.1. Regional Hydrography

Because of the integrated effects of ocean-atmosphere dynamics, the southern YS is influenced by several currents and water masses that are characterized by distinctive seasonal properties: (a) In winter, strong and cold northwest EAWM winds induce southward flowing coastal surface currents, such as the Chinese Coastal Current and Korean Coastal Current which are characterized by low temperature and low salinity (see Figure S1b). As a compensation flow (Figures 1a and S1b), the YSWC, a branch of the Kuroshio Current with a maximum flow velocity at the bottom layer (Tak et al., 2016), flows northward along the western part of the central Yellow Sea Trough and transports warm and salty water sourced from the Kuroshio Current into the YS during the EAWM season (Lin et al., 2011). EAWM winds induce intensive vertical mixing leading to vertical homogeneity of temperatures, whereas the intrusion of YSWC and southward flow of cold coastal currents result in steep latitudinal temperature gradient (Figure 1c). (b) In summer, increased solar radiation heats the surface water resulting in uniformly higher SST in the southern YS (Figure 1b). However, the bottom water in the central trough remains cold (Figure 1d) because a strong vertical temperature gradient prevents a downward heat transfer from the surface to the bottom in the central trough. Therefore, this cold bottom water is called southern Yellow Sea Cold Water Mass which archives the temperature signal of the previous winter season (S. Park et al., 2011) (see Figures 1d and S1b).

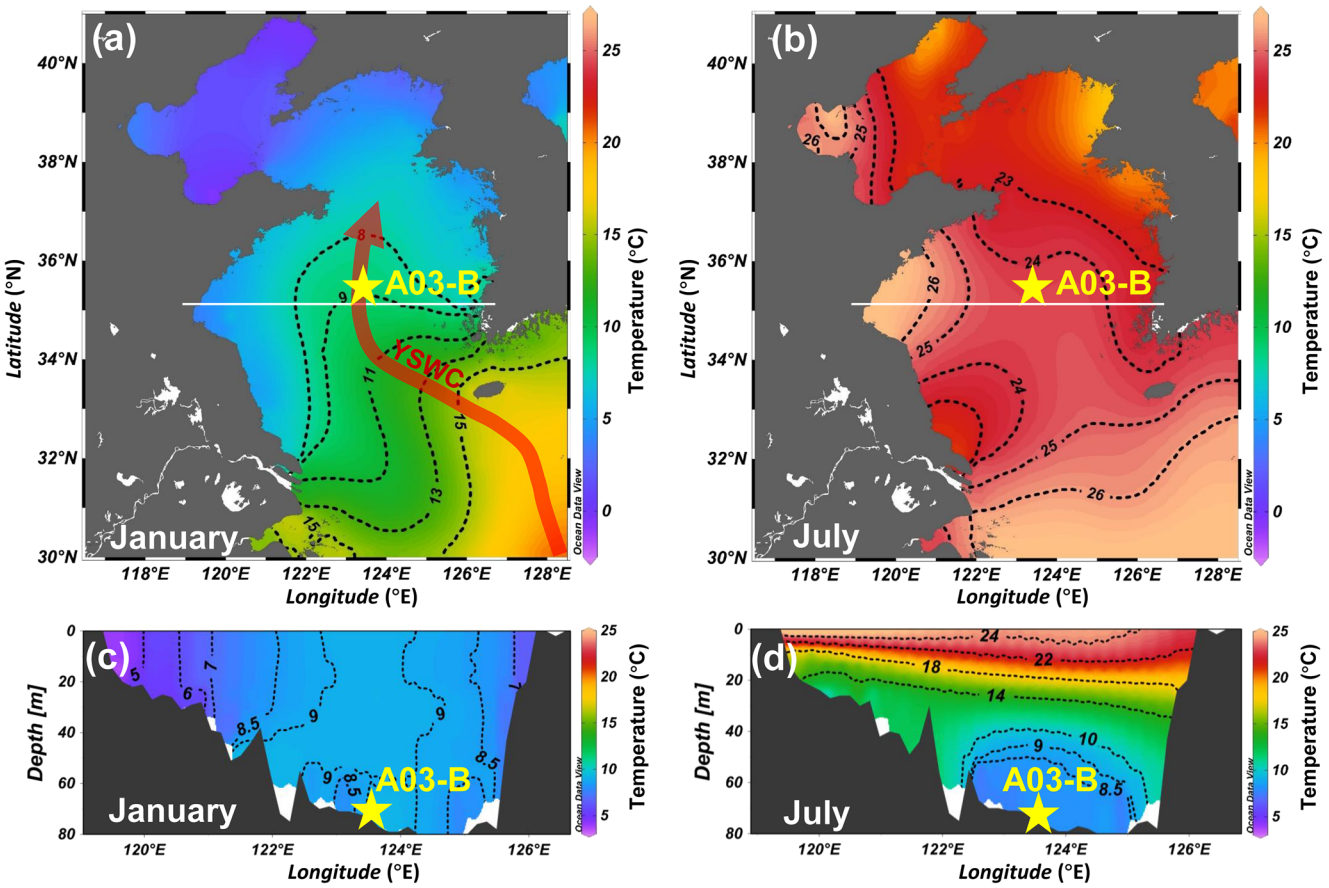

Figure 1. Modern water temperatures at the surface (0 m depth) and temperature transects through the southern Yellow Sea (YS) (white solid line) for January (a), (c) and July (b), (d), respectively. The yellow star indicates the location of core A03-B. Temperature data are from World Ocean Atlas 2013 (https://www.nodc.noaa.gov/OC5/woa13/woa13data.html) for the period 1955–2012 with a 0.25° × 0.25° resolution. YSWC is the Yellow Sea Warm Current. Figures were generated with Ocean Data View software (Schlitzer, 2018).

2.2. Material and Analysis Methods

The age model of core A03-B is based on seven accelerator mass spectrometry (AMS) 14C dates of mixed benthic foraminifera (Jia et al., 2019). AMS 14C dates were converted to calendar ages (B.P., relative to 1950 A.D.) by using the Marine13 data set (Reimer et al., 2013) and a local marine reservoir correction (ΔR) of −128 ± 35 years (Zhong et al., 2018). The used ΔR represents the average of three local ΔR values which are radiocarbon dated Gastropod shells from Qingdao (Southon et al., 2002) and mollusk shells from the Korean peninsula (Kong & Lee, 2005). Core A03-B provides a continuous sedimentary record over the last 8.8 kyr (Figure S2). Sediment core A03-B was sampled at regular 1 cm-intervals for glycerol dibiphytanyl glycerol tetraether analysis (GDGT, see molecular structure in Figure S3), following the procedure described by Y. Wang et al. (2019). Briefly, 2–4 g freeze-dried sediments were homogenized, and ultrasonically extracted four times using a mixture of dichloromethane:methanol (3:1 v/v). Thereafter, the total lipid extracts were concentrated under a N_2 gas stream. After saponified with 6% KOH in methanol for 12 h, the neutral components were extracted with *n*-hexane four times and then separated into apolar and polar fractions by silica gel chromatography using *n*-hexane and dichloromethane:methanol (95:5 v/v), respectively. The polar fraction, which contains the target GDGTs, was then concentrated under N_2 gas stream, re-dissolved in a mixture of *n*-hexane and isopropanol (95:5 v/v), and filtered through a 0.45 μm PTFE filter prior to further analysis.

GDGT analyses were performed on an Agilent 1200 liquid chromatograph equipped with a Waters Micromass-Quattro UltimaTM Pt mass spectrometer (MS) and an atmospheric pressure chemical ionization (APCI) inlet (Schouten et al., 2007). A Prevail Cyano Column (150 × 2.1 mm, 3 μm) maintaining a

temperature of 30°C was used to separate the GDGT components and the elution program with a constant flow rate of 0.2 ml min^{-1} was as follows: *n*-hexane:isopropanol (99:1 v/v) for 5 min initially, then a linear gradient to 2.4% of isopropanol over 25 min, followed by back flushing with *n*-hexane/propanol (99:1 v:v) for 10 min after each sample analysis in order to clean the column. The MS was operated with a corona discharge current at 6 μA, cone voltage at 35 V, APCI probe temperature at 550°C, and the cone gas (N_2) flow at 90 L h^{-1} and the desolvation gas flow at 600 L h^{-1}. Selected Ion Recording (SIR) was used to scan the ($M + H^+$) ions of GDGTs with a dwell time of 237 ms for each ion. GDGT-related parameters were calculated based on the relative abundance of GDGTs.

The average sampling resolution is ~29 yr, which is sufficient to allow multi-centennial time scale reconstruction. The TEX^L_{86} values were calculated according to Kim et al. (2010) (see Equation S1). Duplicate measurements revealed a precision better than 0.5°C for TEX^L_{86}-derived temperature using the southern YS calibration by Xing et al. (2015).

3. Results and Discussion

3.1. YSWC Temperature History

Previous studies reveal that terrestrial sourced isoprenoid GDGTs which have been transported to coastal regions may potentially bias the marine TEX_{86}-temperature (or modified forms) relationship (Weijers et al., 2006; Zhu et al., 2011). The BIT values of 0.034–0.115 (Figure S4a) are lower than 0.3, suggesting that the contribution of terrestrial-derived isoprenoid GDGT is negligible and therefore that the marine TEX_{86}-temperature signal is unlikely biased by the contribution of terrestrial sourced isoprenoid GDGTs (Weijers et al., 2006). Methanogenic Euryarchaeota also produces isoprenoid GDGTs which can bias the TEX_{86} (or modified forms)-temperature relationship (Y. G. Zhang et al., 2011). The MI values of core A03-B range between 0.074 and 0.140 (Figure S4b) and fall within the range of 0–0.3 for non-methanogenic marine archaea. In addition, the (0)/(Cren) values of core A03-B vary between 0.846 and 1.418 (Figure S4c), indicating marine Thaumarchaeota-sourced isoprenoid GDGTs whose (0)/(Cren) ratio is typically <2 (Blaga et al., 2009; Y. G. Zhang et al., 2016). Taken together, the TEX^L_{86} values of core Site A03-B are not affected by non-thermal factors. Using the local southern YS TEX^L_{86}-BWT calibration (Xing et al., 2015), TEX^L_{86}-derived BWT of the A03-B core-top sample (0–1 cm, with an age of ~37 yr BP) is 9.0°C (Figure 2a), which is close to the depth-integrated (45–65 m) annual mean temperature of 8.7 ± 0.4°C at A03-B site (Figure S5), providing further evidence that the TEX^L_{86} index records bottom water temperatures (also see discussion in supporting information).

3.2. Mechanisms Controlling Southern YS Temperature Changes

3.2.1. Long-Term Trend

BWTs at core Site A03-B varies between 8.3°C and 13.1°C during the last 8.8 kyr (Figures 2a and S5). The most striking feature of our BWT record is a gradual long-term cooling trend of ~3.0°C from ~5 kyr BP to the core top (Figure 2a). Modern surveys reveal that southern Yellow Sea Cold Water Mass is a remnant of cold, vertically well-mixed water of the previous winter (Figures 1 and S5). For that reason, BWTs at site A03-B is tightly coupled with the temperature of the winter season YSWC. The temperature of the YSWC is affected by winter surface cooling and by mixing of cold YS water with warm Kuroshio Current water. The temperature of the Kuroshio Current is governed by the heat content of the WPWP (Wu et al., 2012 and references therein). Modern observations and numerical model simulations reveal that the EAWM modulates the northward propagation of the YSWC (Lin et al., 2011; Tak et al., 2016). On the one hand, a stronger (weaker) EAWM increases (decreases) the northward intrusion of warm and salty water into the southern YS. On the other hand, the EAWM brings cold air from the Eurasia which reduces the YS water temperatures through air-sea interaction. Both proxy records and model simulation results suggest that the intensity of the EAWM wind over the northern East Asian marginal seas increased gradually from the middle to the late Holocene (Figure S7) (Hao et al., 2017; Kang et al., 2020; Yancheva et al., 2007; Zhao et al., 2019), leading to an increased low-latitude source water intrusion into the southern YS as inferred from the increased salinity of the southern Yellow Sea Cold Water Mass (T. Li et al., 2009; Xiang et al., 2008). Therefore, a gradual increase in BWTs at core Site A03-B is expected due to an increased mixing ratio of

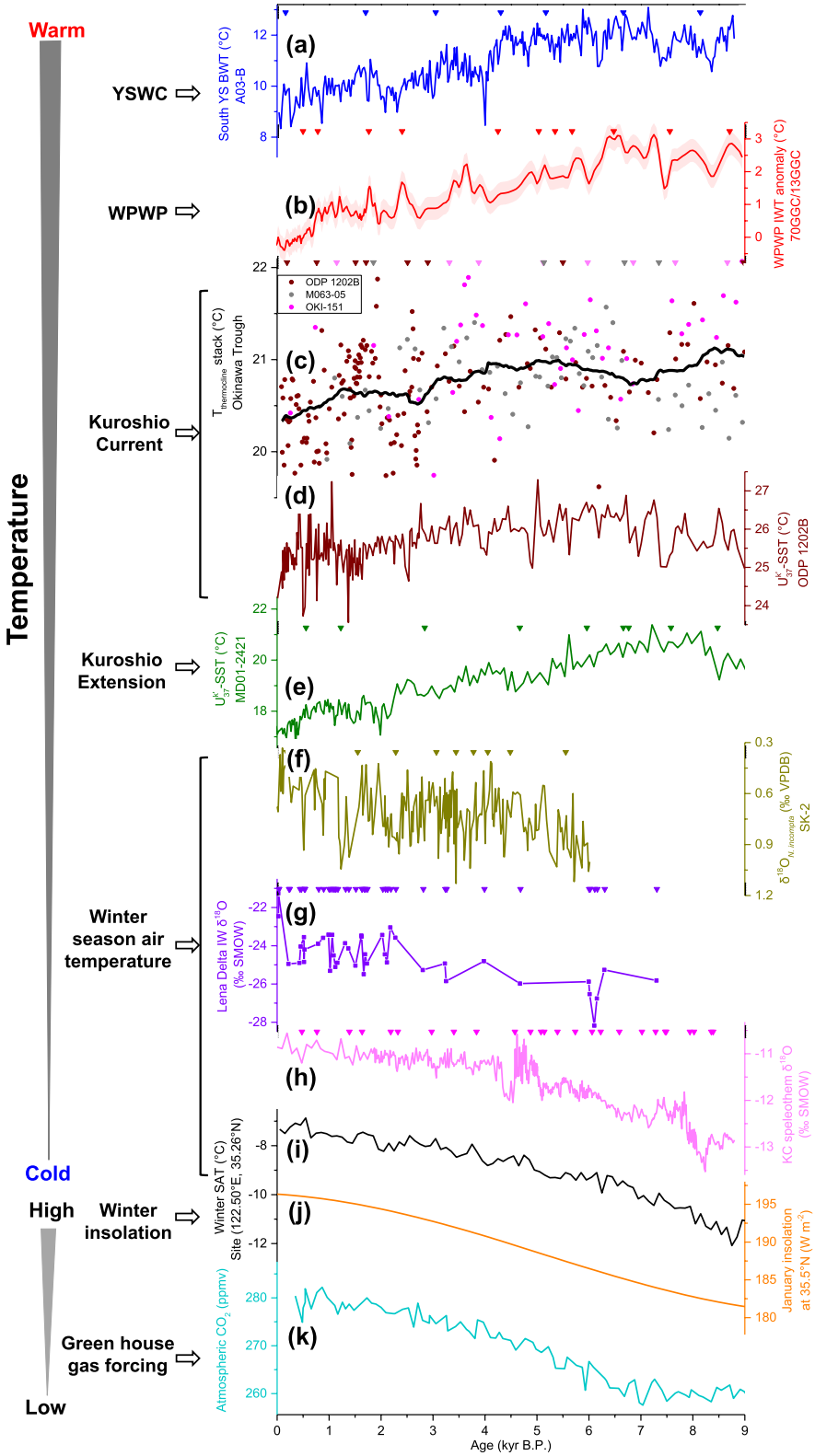
Warm
Cold
Temperature
High
Low
YSWC
WPWP
Kuroshio Current
Kuroshio Extension
Winter season air temperature
Winter insolation
Green house gas forcing
(a)
(b)
(c)
(d)
(e)
(f)
(g)
(h)
(i)
(j)
(k)
South YS BWT (°C) A03-B
WPWP IWT anomaly (°C) 70GGC/13GGC
ODP 1202B
M063-05
OKI-151
T thermocline stack (°C) Okinawa Trough
U37K'-SST (°C) ODP 1202B
U37K'-SST (°C) MD01-2421
δ18O N. incompta (‰ VPDB) SK-2
Lena Delta IW δ18O (‰ SMOW)
KC speleothem δ18O (‰ SMOW)
Winter SAT (°C) Site (122.50°E, 35.26°N)
January insolation at 35.5°N (W m-2)
Atmospheric CO2 (ppmv)
Age (kyr B.P.)

low-latitude warm water from the middle to the late Holocene. However, the cooling trend of our BWT do not support this scenario (Figures 2a and S7), ruling out EAWM driven water mixing as the primary factor which controls BWT changes in the southern YS (also see discussion in supporting information).

Both paleo-proxy records (Figures 2f, 2g, and 2h) and climate model simulations (TraCE-21ka, Figure 2i) have revealed a gradual warming of the Northern Hemisphere winter air temperature since the middle Holocene, in response to an increase in winter insolation and/or greenhouse gases (Figures 2j and 2k) (Baker et al., 2017; Liu et al., 2009; Meyer et al., 2015; Sagawa et al., 2014). This is contrast to the cooling trend observed in our BWT record, which excludes the top-down atmospheric forcing through surface cooling to explain the BWT changes in the southern YS. Today, water temperature of the YSWC shows similar changes with air temperature prevailing over the southern YS during the winter season (Figure S8). The different responses of the YSWC water temperature to winter season air temperature between modern observation and paleo-records suggest that mechanisms controlling the YSWC temperature change are different on annual-to-decadal timescales and on sub-orbital timescale.

Another influence on the YSWC temperature could be a water temperature change of the YSWC source water itself. As shown in Figure 2, there exists a good positive correlation ($r = 0.83$, $p < 0.05$) between the southern YS BWT and the WPWP intermediate water temperature. We therefore suggest that the cooling of the low-latitude source waters from the middle to late Holocene is likely responsible for the decrease in BWTs in the southern YS. Temperature reconstructions of intermediate waters (500–600 m water depth) in the WPWP have revealed a cooling of 2.1 ± 0.4°C during the mid-to-late Holocene (Rosenthal et al., 2013). The cooling of the intermediate waters is accompanied by a cooling of the WPWP thermocline (Dang et al., 2020) and surface water temperatures (Linsley et al., 2010), a contraction of the WPWP (Moffa-Sanchez et al., 2019) and a southward shift of Kuroshio extension (Isono et al., 2009). The concordant decrease of the BWTs in the southern YS and intermediate/thermocline water temperatures in the WPWP might imply that the temperature signal of the low-latitude source waters was transmitted by the Kuroshio Current, which flows northward along the western side of the Okinawa Trough and carries large amounts of heat (and temperature signal) from the tropics to mid-latitudes (Wu et al., 2012 and references therein), into the YS (Figures 2a–2d) via its intermediate/thermocline waters. Upwelling of the Kuroshio intermediate/thermocline waters along the East China Sea shallow continental slope forms the YSWC and therefore brings the tropical subsurface water temperature signal into the southern YS during winter season (Figure S9). Alternatively, as the WPWP cooled and contracted, the Kuroshio Current intensity decreased gradually during the middle to late Holocene (Q. Li et al., 2019; Zheng et al., 2016), which further amplified this northward low-latitude source cooling signal. Although Kuroshio Current intermediate water temperature records are not available to test this most likely scenario, TEX_{86} derived thermocline/subsurface temperature records provide some support for the proposed scenario. As shown in Figure 2c, TEX_{86}-derived temperature records from the Okinawa Trough (Q. Li et al., 2020; Ruan et al., 2017; Xu et al., 2018) and East China Sea (Yuan et al., 2018) reveal a gradual cooling since ~5 ka. The concurrent SST cooling in the Okinawa Trough (Figure 2d) (Ruan et al., 2015) and BTW cooling in the southern YS most likely suggests that the Kuroshio Current transmitted the WPWP cooling signal into the YS.

Figure 2. Temporal variations of bottom water temperatures in the Yellow Sea (YS) compared to other paleo-records. (a) TEX^{L}_{86} derived bottom water temperature (BWT) from core A03-B (this study). (b) Western Pacific Warm Pool (WPWP) intermediate water temperature (IWT) anomaly estimated from Mg/Ca-based temperatures of benthic foraminifera *Hyalinea balthica* from cores 70GGC and 13GGC (Rosenthal et al., 2013). (c) Okinawa Trough thermocline/subsurface temperature stack (black line) based on TEX_{86}-temperatures from sites ODP 1202B (Ruan et al., 2017), M063-05 (Q. Li et al., 2020), and OKI-151 (Xu et al., 2018). TEX_{86}-derived thermocline temperatures were calculated by using the TEX_{86}-temperature equation by Kim et al. (2012). (d) Alkenone-derived sea surface temperature ($U^{k'}_{37}$-SST) estimates from site ODP 1202B (Ruan et al., 2015). (e) Alkenone-derived sea surface temperature ($U^{k'}_{37}$-SST) estimates from site MD01-2421 which is located in the extension of the Kuroshio Current (Isono et al., 2009). (f) $\delta^{18}O_{N.\ incompta}$ from site SK-2 off Japan (Sagawa et al., 2014). (g) $\delta^{18}O$ of permafrost ice wedges (IW) from the Lena River Delta in the Siberian Arctic (Meyer et al., 2015). (h) Stalagmite $\delta^{18}O$ from Kinderlinskaya Cave in the southern Ural Mountains of Russia (Baker et al., 2017). (i) Model results of surface air temperature during the winter season (December-February) at site (122.50°E, 35.26°N) close to core A03-B. Model simulation data are from Liu et al. (2009) (http://202.195.239.65:8888/). (j) January insolation at 35.5°N (Laskar et al., 2004). (k) Composite record of atmospheric CO_2 from Antarctic ice cores (Bereiter et al., 2015). AMS ^{14}C age-control points are indicated by triangles above each record. EAWM, East Asia winter monsoon; YSWC, Yellow Sea Warm Current.

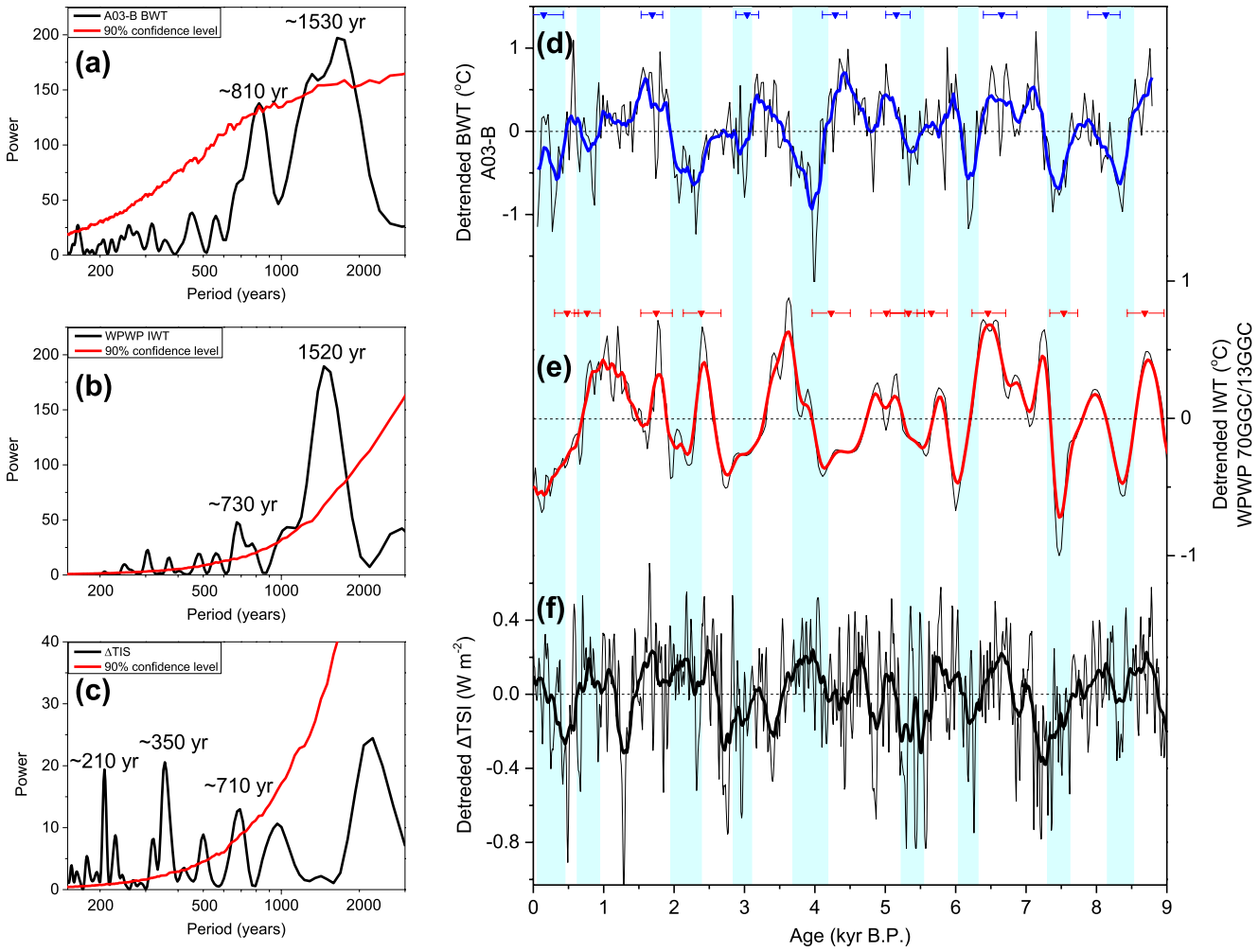

Figure 3. Spectral analyses of paleo-records and variations in the detrended time series. (a), (b), and (c) are spectral analyses of bottom water temperature (BWT) of core A03-B (this study), Western Pacific Warm Pool (WPWP) intermediate water temperature (IWT) (Rosenthal et al., 2013) and the total solar irradiance (TSI) obtained from the cosmogenic radionuclide ^{10}Be measured in ice cores (Steinhilber et al., 2009), respectively. The REDFIT3.8e software of Schulz and Mudelsee (2002) was used for spectral analyses. Red lines represent 90% confidence level from Monte-Carlo simulations. (d) Detrended BWT at core A03-B (this study). (e) Detrended ITW of WPWP (Rosenthal et al., 2013). (f) Detrended TSI (Steinhilber et al., 2009). Detrended data were calculated by subtract 2,500 yr running mean from raw data. Solid lines in (d), (e) and (f) are 200 yr running mean. Blue and red triangles are the AMS ^{14}C age-control points for cores A03-B (Jia et al., 2019) and 70GGC/13GGC (Rosenthal et al., 2013), respectively. Light blue bars indicate cold periods in the A03-B record.

3.2.2. Multi-Centennial- and Millennial-Scale Variability

Superimposed on the long term BWT cooling trend at core A03-B are rapid fluctuations with amplitudes of ~1–2°C (Figures 2a and 3d). Spectral analysis indicates BWT variability at multi-centennial and millennial timescales with periodicities of ~810 and ~1,530 yr (>90% confidence level) (Figure 3a), similar to the periodicities of ~730 and ~1,520 yr, respectively, identified in the WPWP intermediate water record (Figure 3b). We further explore the relationship between southern YS BWT and WPWP intermediate water temperature variability by using band-pass filters (650–850 years and 1,400–1,600 years) corresponding to the spectral peaks. Figure S10 reveal that the two records share common multi-centennial and millennial changes, especially prominent on the 650–850 years filter. Uncertainties associated with the individual age models (2σ range of 150–350 years, Figure 3) however prevent any significant phase comparison between two data series. The detrended time series reveal that those multi-centennial and millennial scale BWT changes coincide with intermediate water variations in the WPWP (Figures 3d and 3e). We suggest the same mechanism above to explain those short scale BTW variations in the southern YS. In addition, the ~700–800

and ~1,500 yr periodicities have been also identified in a proxy record for changes in the Kuroshio Current intensity during the Holocene (Jian et al., 2000), supporting our scenario to explain the YS BTW changes.

The $\delta^{18}O_{N.\ incompta}$ record of core Site SK-2 near Japan has been proposed to reflect winter season temperature changes which are tightly connected with EAWM changes (Sagawa et al., 2014). Spectral analysis indicates a significant periodicity of ~750 yr in the $\delta^{18}O$ record (Figure S11a). However, there is only a weak correlation between the BWT at core Site A03-B and the SK-2 $\delta^{18}O_{N.\ incompta}$ record (Figure S11) which also lacks the ~1,500 yr periodicity (Sagawa et al., 2014). We therefore suggest that the impact of winter season surface cooling on the YSWC water temperature would have been only minor at multi-centennial and millennial timescales.

The ~700–800 and ~1,500 year spectral signals have been found in both the southern YS BWT and the WPWP intermediate water temperature and have also been observed in other Holocene records from the western Pacific (Hao et al., 2017; Isono et al., 2009; Jian et al., 2000; Khider et al., 2014; J. Park, 2017; Sagawa et al., 2014), and the Atlantic (Debret et al., 2009 and references therein). The ~700–800 year periodicity could be attributed to external (solar) forcing (Figure 3c) through the amplification by the El Niño-Southern Oscillation (Emile-Geay et al., 2007; Marchitto et al., 2010) or by high latitude regions with further equatorward transport by oceanic thermohaline circulation (Rosenthal et al., 2013). The ~1,500 year periodicity has been attributed to internal forcing, including ocean circulation and/or an ocean/atmosphere coupling (Debret et al., 2009 and references therein). Whatever the main mechanism is, our results reveal that the Kuroshio Current could bridge the meridional heat content between tropical and mid-latitude regions (Figure S9), implying a key role of the tropical intermediate water heat content changes in regulating subtropical ocean dynamics and climate during the mid-to-late Holocene.

4. Conclusions and Implications

Archeal membrane lipid-based proxy derived BTW record reveals multi-centennial-scale changes superimposed on a progressive cooling trend (~5 ka to the present) of the YSWC during the mid-to-late Holocene. We show for the first time that YSWC temperature changes are positively correlated to the evolution of subsurface water temperature variability in the Western Pacific Warm Pool on multi-centennial- to multi-millennial-timescales. We proposed that Kuroshio Current transmitted this tropical ocean thermodynamic signal into the southern YS. In order to support our findings, further studies on the centennial-scale temperature evolution of Kuroshio Current intermediate water are certainly needed to validate our interpretation.

Furthermore, the observed temperature coupling between YSWC and WPWP intermediate water may shed new light on our prediction about the consequence of future global warming in the marginal seas of China. In the past two millennia, reconstructed intermediate water temperature closely follows the overlying SST changes in the WPWP with a time lag of multi-decadal to centennial years (Rosenthal et al., 2013). For example, over the past 100 years, SSTs of the WPWP warmed and returned to levels of the Medieval Warm Period (MWP, 950–1250 CE), whereas reconstructed intermediate water temperatures of the WPWP were about the same as that of the Little Ice Age (LIA, 1550–1850 CE), 0.9 ± 0.3°C colder than during the MWP (Rosenthal et al., 2013). The difference suggests that the WPWP intermediate water temperature is not in equilibrium with the recent climate change, for example, anthropogenic greenhouse gases emission forcing. Therefore, we propose that the southern YS bottom water may experience significant warming in the near future if the continuous emissions of anthropogenic greenhouse gases co-occurs with the recovery of WPWP intermediate water temperature from LIA level.

Data Availability Statement

All of the original data have been uploaded as supporting information and deposited publicly to the repository of Zenodo (https://doi.org/10.5281/zenodo.4747779). All the supporting data can be found in the cited references (Baker et al., 2017; Bereiter et al., 2015; Hao et al., 2017; Isono et al., 2009; Kang et al., 2020; Laskar et al., 2004; Q. Li et al., 2020; Liu et al., 2009; Meyer et al., 2015; Rosenthal et al., 2013; Ruan et al., 2015, 2017; Sagawa et al., 2014; Steinhilber et al., 2009; Xu et al., 2018; Yancheva et al., 2007; Zhao et al., 2019; Zheng et al., 2014).

Acknowledgments
The authors thank Prof. Liping Zhou (Peking University), Prof. H. Yan (Institute of Earth Environment, Chinese Academy of Sciences) and Dr. Y. Ding (Ocean University of China) for constructive discussions. The authors sincerely appreciate the time and effort provided by two anonymous reviewers to improve this paper. This study was supported by the National Natural Science Foundation of China (Grants 41876076, 91958104, and 41630966) and by the Fundamental Research Funds for the Central Universities (Grants 202041007 and 201813029). This is MCTL contribution #239.

References

Baker, J. L., Lachniet, M. S., Chervyatsova, O., Asmerom, Y., & Polyak, V. J. (2017). Holocene warming in western continental Eurasia driven by glacial retreat and greenhouse forcing. *Nature Geoscience*, *10*(6), 430–435. https://doi.org/10.1038/ngeo2953

Bereiter, B., Eggleston, S., Schmitt, J., Nehrbass-Ahles, C., Stocker, T. F., Fischer, H., et al. (2015). Revision of the EPICA Dome C CO_2 record from 800 to 600 kyr before present. *Geophysical Research Letters*, *42*(2), 542–549. https://doi.org/10.1002/2014gl061957

Blaga, C. I., Reichart, G.-J., Heiri, O., & Sinninghe Damsté, J. S. (2009). Tetraether membrane lipid distributions in water-column particulate matter and sediments: A study of 47 European lakes along a north-south transect. *Journal of Paleolimnology*, *41*(3), 523–540. https://doi.org/10.1007/s10933-008-9242-2

Dang, H., Jian, Z., Wang, Y., Mohtadi, M., Rosenthal, Y., Ye, L., et al. (2020). Pacific warm pool subsurface heat sequestration modulated Walker circulation and ENSO activity during the Holocene. *Science Advance*, *6*(42), eabc0402. https://doi.org/10.1126/sciadv.abc0402

Debret, M., Sebag, D., Crosta, X., Massei, N., Petit, J.-R., Chapron, E., & Bout-Roumazeilles, V. (2009). Evidence from wavelet analysis for a mid-Holocene transition in global climate forcing. *Quaternary Science Reviews*, *28*(25), 2675–2688. https://doi.org/10.1016/j.quascirev.2009.06.005

Emile-Geay, J., Cane, M., Seager, R., Kaplan, A., & Almasi, P. (2007). El Niño as a mediator of the solar influence on climate. *Paleoceanography*, *22*(3), PA3210. https://doi.org/10.1029/2006PA001304

Hao, T., Liu, X., Ogg, J., Liang, Z., Xiang, R., Zhang, X., et al. (2017). Intensified episodes of east Asian Winter monsoon during the middle through late Holocene driven by north Atlantic cooling events: High-resolution lignin records from the South Yellow Sea, China. *Earth and Planetary Science Letters*, *479*, 144–155. https://doi.org/10.1016/j.epsl.2017.09.031

Isono, D., Yamamoto, M., Irino, T., Oba, T., Murayama, M., Nakamura, T., & Kawahata, H. (2009). The 1500-year climate oscillation in the midlatitude north Pacific during the Holocene. *Geology*, *37*(7), 591–594. https://doi.org/10.1130/G25667A.1

Jia, Y., Li, D.-W., Yu, M., Zhao, X., Xiang, R., Li, G., et al. (2019). High- and low-latitude forcing on the south Yellow Sea surface water temperature variations during the Holocene. *Global and Planetary Change*, *182*, 103025. https://doi.org/10.1016/j.gloplacha.2019.103025

Jian, Z., Wang, P., Saito, Y., Wang, J., Pflaumann, U., Oba, T., & Cheng, X. (2000). Holocene variability of the Kuroshio Current in the Okinawa Trough, northwestern Pacific Ocean. *Earth and Planetary Science Letters*, *184*(1), 305–319. https://doi.org/10.1016/S0012-821X(00)00321-6

Kang, S., Du, J., Wang, N., Dong, J., Wang, D., Wang, X., et al. (2020). Early Holocene weakening and mid- to late Holocene strengthening of the east Asian winter monsoon. *Geology*, *48*(11), 1043–1047. https://doi.org/10.1130/g47621.1

Khider, D., Jackson, C. S., & Stott, L. D. (2014). Assessing millennial-scale variability during the Holocene: A perspective from the western tropical Pacific. *Paleoceanography*, *29*(3), 143–159. https://doi.org/10.1002/2013PA002534

Kim, J.-H., Romero, O. E., Lohmann, G., Donner, B., Laepple, T., Haam, E., & Sinninghe Damsté, J. S. (2012). Pronounced subsurface cooling of north Atlantic waters off northwest Africa during Dansgaard-Oeschger interstadials. *Earth and Planetary Science Letters*, *339–340*, 95–102. https://doi.org/10.1016/j.epsl.2012.05.018

Kim, J.-H., van der Meer, J., Schouten, S., Helmke, P., Willmott, V., Sangiorgi, F., et al. (2010). New indices and calibrations derived from the distribution of crenarchaeal isoprenoid tetraether lipids: Implications for past sea surface temperature reconstructions. *Geochimica et Cosmochimica Acta*, *74*(16), 4639–4654. https://doi.org/10.1016/j.gca.2010.05.027

Kong, G. S., & Lee, C. W. (2005). Marine reservoir corrections (ΔR) for southern coastal waters of Korea. *The Korean Society of Oceanography*, *2*, 124–128.

Laskar, J., Robutel, P., Joutel, F., Gastineau, M., Correia, A. C. M., & Levrard, B. (2004). A long-term numerical solution for the insolation quantities of the Earth. *Astronomy & Astrophysics*, *428*(1), 261–285. https://doi.org/10.1051/0004-6361:20041335

Li, Q., Li, G., Chen, M. T., Xu, J., Liu, S., & Chen, M. (2020). New insights into Kuroshio current evolution since the last deglaciation based on paired organic paleothermometers from the middle Okinawa Trough. *Paleoceanography and Paleoclimatology*, *35*(12), e2020PA004140. https://doi.org/10.1029/2020PA004140

Li, Q., Zhang, Q., Li, G., Liu, Q., Chen, M.-T., Xu, J., & Li, J. (2019). A new perspective for the sediment provenance evolution of the middle Okinawa Trough since the last deglaciation based on integrated methods. *Earth and Planetary Science Letters*, *528*, 115839. https://doi.org/10.1016/j.epsl.2019.115839

Li, T., Nan, Q., Jiang, B., Sun, R., Zhang, D., & Li, Q. (2009). Formation and evolution of the modern warm current system in the east China Sea and the Yellow Sea since the last deglaciation. *Chinese Journal of Oceanology and Limnology*, *27*(2), 237–249. https://doi.org/10.1007/s00343-009-9149-4

Lin, X., Yang, J., Guo, J., Zhang, Z., Yin, Y., Song, X., & Zhang, X. (2011). An asymmetric upwind flow, Yellow Sea Warm Current: 1. New observations in the western Yellow Sea. *Journal of Geophysical Research*, *116*(C4), C04026. https://doi.org/10.1029/2010jc006513

Linsley, B. K., Rosenthal, Y., & Oppo, D. W. (2010). Holocene evolution of the Indonesian throughflow and the western Pacific warm pool. *Nature Geoscience*, *3*(8), 578–583. https://doi.org/10.1038/ngeo920

Liu, Z., Otto-Bliesner, B. L., He, F., Brady, E. C., Tomas, R., Clark, P. U., et al. (2009). Transient simulation of last deglaciation with a new mechanism for Bolling-Allerod warming. *Science*, *325*(5938), 310–314. https://doi.org/10.1126/science.1171041

Marchitto, T. M., Muscheler, R., Ortiz, J. D., Carriquiry, J. D., & van Geen, A. (2010). Dynamical response of the tropical Pacific Ocean to solar forcing during the early Holocene. *Science*, *330*(6009), 1378–1381. https://doi.org/10.1126/science.1194887

Meyer, H., Opel, T., Laepple, T., Dereviagin, A. Y., Hoffmann, K., & Werner, M. (2015). Long-term winter warming trend in the Siberian Arctic during the mid- to late Holocene. *Nature Geoscience*, *8*(2), 122–125. https://doi.org/10.1038/ngeo2349

Moffa-Sanchez, P., Rosenthal, Y., Babila, T. L., Mohtadi, M., & Zhang, X. (2019). Temperature evolution of the Indo-Pacific warm pool over the Holocene and the last deglaciation. *Paleoceanography and Paleoclimatology*, *34*(7), 1107–1123. https://doi.org/10.1029/2018PA003455

Nan, Q., Li, T., Chen, J., Chang, F., Yu, X., Xu, Z., & Pi, Z. (2017). Holocene paleoenvironment changes in the northern Yellow Sea: Evidence from alkenone-derived sea surface temperature. *Palaeogeography, Palaeoclimatology, Palaeoecology*, *483*, 83–93. https://doi.org/10.1016/j.palaeo.2017.01.031

Park, J. (2017). Solar and Tropical Ocean forcing of late-Holocene climate change in coastal East Asia. *Palaeogeography, Palaeoclimatology, Palaeoecology*, *469*, 74–83. https://doi.org/10.1016/j.palaeo.2017.01.005

Park, S., Chu, P. C., & Lee, J.-H. (2011). Interannual-to-interdecadal variability of the Yellow Sea Cold Water Mass in 1967–2008: Characteristics and seasonal forcings. *Journal of Marine Systems*, *87*(3), 177–193. https://doi.org/10.1016/j.jmarsys.2011.03.012

Reimer, P. J., Bard, E., Bayliss, A., Beck, J. W., Blackwell, P. G., Ramsey, C. B., et al. (2013). IntCal13 and Marine13 radiocarbon age calibration curves 0–50,000 years cal BP. *Radiocarbon*, *55*(4), 1869–1887. https://doi.org/10.2458/azu_js_rc.55.16947

Rosenthal, Y., Linsley, B. K., & Oppo, D. W. (2013). Pacific Ocean heat content during the past 10,000 years. *Science*, *342*(6158), 617–621. https://doi.org/10.1126/science.1240837

Ruan, J., Xu, Y., Ding, S., Wang, Y., & Zhang, X. (2015). A high resolution record of sea surface temperature in southern Okinawa Trough for the past 15,000 years. *Palaeogeography, Palaeoclimatology, Palaeoecology*, *426*(0), 209–215. https://doi.org/10.1016/j.palaeo.2015.03.007

Ruan, J., Xu, Y., Ding, S., Wang, Y., & Zhang, X. (2017). A biomarker record of temperature and phytoplankton community structure in the Okinawa Trough since the last glacial maximum. *Quaternary Research*, *88*(1), 89–97. https://doi.org/10.1017/qua.2017.28

Sagawa, T., Kuwae, M., Tsuruoka, K., Nakamura, Y., Ikehara, M., & Murayama, M. (2014). Solar forcing of centennial-scale east Asian winter monsoon variability in the mid- to late Holocene. *Earth and Planetary Science Letters*, *395*(0), 124–135. https://doi.org/10.1016/j.epsl.2014.03.043

Schlitzer, R. (2018). *Ocean data view*. Retrieved from https://odv.awi.de

Schouten, S., Huguet, C., Hopmans, E. C., Kienhuis, M. V. M., & Sinninghe Damsté, J. S. (2007). Analytical methodology for TEX86 paleothermometry by high-performance liquid chromatography/atmospheric pressure chemical ionization-mass spectrometry. *Analytical Chemistry*, *79*(7), 2940–2944. https://doi.org/10.1021/ac062339v

Schulz, M., & Mudelsee, M. (2002). REDFIT: Estimating red-noise spectra directly from unevenly spaced paleoclimatic time series. *Computers & Geosciences*, *28*, 421–426. https://doi.org/10.1016/S0098-3004(01)00044-9

Solomon, A., & Newman, M. (2012). Reconciling disparate twentieth-century Indo-Pacific ocean temperature trends in the instrumental record. *Nature Climate Change*, *2*(9), 691–699. https://doi.org/10.1038/nclimate1591

Southon, J., Kashgarian, M., Fontugne, M., Metivier, B., & Yim, W. W-S. (2002). Marine reservoir corrections for the Indian Ocean and southeast Asia. *Radiocarbon*, *44*(1), 167–180. https://doi.org/10.1017/S0033822200064778

Steinhilber, F., Beer, J., & Fröhlich, C. (2009). Total solar irradiance during the Holocene. *Geophysical Research Letters*, *36*(19), L19704. https://doi.org/10.1029/2009gl040142

Sun, Y., Clemens, S. C., Morrill, C., Lin, X., Wang, X., & An, Z. (2012). Influence of Atlantic meridional overturning circulation on the east Asian winter monsoon. *Nature Geoscience*, *5*(1), 46–49. https://doi.org/10.1038/ngeo1326

Tak, Y. J., Cho, Y. K., Seo, G. H., & Choi, B. J. (2016). Evolution of wind-driven flows in the Yellow Sea during winter. *Journal of Geophysical Research: Oceans*, *121*(3), 1970–1983. https://doi.org/10.1002/2016jc011622

Wang, L., Yang, Z., Zhang, R., Fan, D., Zhao, M., & Hu, B. (2011). Sea surface temperature records of core ZY2 from the central mud area in the south Yellow Sea during last 6200 years and related effect of the Yellow Sea Warm Current. *Chinese Science Bulletin*, *56*(15), 1588–1595. https://doi.org/10.1007/s11434-011-4442-y

Wang, Y., Li, D.-W., Sachs, J. P., Hu, J., Cao, Y., Li, L., et al. (2019). Vertical distribution of isoprenoid GDGTs in suspended particles from the east China Sea shelf and implications for sedimentary TEX86H records. *Organic Geochemistry*, *136*, 103895. https://doi.org/10.1016/j.orggeochem.2019.07.004

Wanner, H., Solomina, O., Grosjean, M., Ritz, S. P., & Jetel, M. (2011). Structure and origin of Holocene cold events. *Quaternary Science Reviews*, *30*(21), 3109–3123. https://doi.org/10.1016/j.quascirev.2011.07.010

Weijers, J. W. H., Schouten, S., Spaargaren, O. C., & Sinninghe Damsté, J. S. (2006). Occurrence and distribution of tetraether membrane lipids in soils: Implications for the use of the TEX86 proxy and the BIT index. *Organic Geochemistry*, *37*(12), 1680–1693. https://doi.org/10.1016/j.orggeochem.2006.07.018

Wu, L., Cai, W., Zhang, L., Nakamura, H., Timmermann, A., Joyce, T., et al. (2012). Enhanced warming over the global subtropical western boundary currents. *Nature Climate Change*, *2*(3), 161–166. https://doi.org/10.1038/nclimate1353

Xiang, R., Yang, Z., Saito, Y., Fan, D., Chen, M., Guo, Z., & Chen, Z. (2008). Paleoenvironmental changes during the last 8400 years in the southern Yellow Sea: Benthic foraminiferal and stable isotopic evidence. *Marine Micropaleontology*, *67*(1), 104–119. https://doi.org/10.1016/j.marmicro.2007.11.002

Xing, L., Sachs, J. P., Gao, W., Tao, S., Zhao, X., Li, L., et al. (2015). TEX 86 paleothermometer as an indication of bottom water temperature in the Yellow Sea. *Organic Geochemistry*, *86*, 19–31. https://doi.org/10.1016/j.orggeochem.2015.05.007

Xu, F., Dou, Y., Li, J., Cai, F., Zhao, J., Wen, Z., et al. (2018). Low-latitude climate control on sea-surface temperatures recorded in the southern Okinawa Trough during the last 13.3 kyr. *Palaeogeography, Palaeoclimatology, Palaeoecology*, *490*, 210–217. https://doi.org/10.1016/j.palaeo.2017.10.034

Yancheva, G., Nowaczyk, N. R., Mingram, J., Dulski, P., Schettler, G., Negendank, J. F. W., et al. (2007). Influence of the intertropical convergence zone on the east Asian monsoon. *Nature*, *445*(7123), 74–77. https://doi.org/10.1038/nature05431

Yuan, Z., Xiao, X., Wang, F., Xing, L., Wang, Z., Zhang, H., et al. (2018). Spatiotemporal temperature variations in the east China Sea shelf during the Holocene in response to surface circulation evolution. *Quaternary International*, *482*, 46–55. https://doi.org/10.1016/j.quaint.2018.04.025

Zhang, Y., Zhou, X., He, Y., Jiang, Y., Liu, Y., Xie, Z., et al. (2019). Persistent intensification of the Kuroshio Current during late Holocene cool intervals. *Earth and Planetary Science Letters*, *506*, 15–22. https://doi.org/10.1016/j.epsl.2018.10.018

Zhang, Y. G., Pagani, M., & Wang, Z. (2016). Ring index: A new strategy to evaluate the integrity of TEX86 paleothermometry. *Paleoceanography*, *31*(2), 220–232. https://doi.org/10.1002/2015PA002848

Zhang, Y. G., Zhang, C. L., Liu, X.-L., Li, L., Hinrichs, K.-U., & Noakes, J. E. (2011). Methane index: A tetraether archaeal lipid biomarker indicator for detecting the instability of marine gas hydrates. *Earth and Planetary Science Letters*, *307*(3–4), 525–534. https://doi.org/10.1016/j.epsl.2011.05.031

Zhao, D., Wan, S., Song, Z., Gong, X., Zhai, L., Shi, X., & Li, A. (2019). Asynchronous variation in the quaternary east Asian winter monsoon associated with the tropical pacific ENSO-like system. *Geophysical Research Letters*, *46*(12), 6955–6963. https://doi.org/10.1029/2019GL083033

Zheng, X., Li, A., Kao, S., Gong, X., Frank, M., Kuhn, G., et al. (2016). Synchronicity of Kuroshio Current and climate system variability since the Last Glacial Maximum. *Earth and Planetary Science Letters*, *452*, 247–257. https://doi.org/10.1016/j.epsl.2016.07.028

Zheng, X., Li, A., Wan, S., Jiang, F., Kao, S. J., & Johnson, C. (2014). ITCZ and ENSO pacing on east Asian winter monsoon variation during the Holocene: Sedimentological evidence from the Okinawa Trough. *Journal of Geophysical Research: Oceans*, *119*(7), 4410–4429. https://doi.org/10.1002/2013JC009603

Zhong, F., Xiang, R., Yang, Y., & Zhao, M. (2018). Evolution of the southern Yellow Sea Cold Water Mass during the last 7 kyr from benthic foraminiferal evidence. *Science China Earth Sciences*, *61*(10), 1406–1418. https://doi.org/10.1007/s11430-017-9193-6

Zhu, C., Weijers, J. W. H., Wagner, T., Pan, J.-M., Chen, J.-F., & Pancost, R. D. (2011). Sources and distributions of tetraether lipids in surface sediments across a large river-dominated continental margin. *Organic Geochemistry*, *42*(4), 376–386. https://doi.org/10.1016/j.orggeochem.2011.02.002

References From the Supporting Information

Blaauw, M., & Christen, J. A. (2011). Flexible paleoclimate age-depth models using an autoregressive gamma process. *Bayesian Analysis*, *6*, 457–474. https://doi.org/10.1214/11-BA61810.1214/ba/1339616472

Hopmans, E. C., Weijers, J. W. H., Schefuß, E., Herfort, L., Sinninghe Damsté, J. S., & Schouten, S. (2004). A novel proxy for terrestrial organic matter in sediments based on branched and isoprenoid tetraether lipids. *Earth and Planetary Science Letters*, *224*(1–2), 107–116. https://doi.org/10.1016/j.epsl.2004.05.012

Hsiao, S. S.-Y., Hsu, T.-C., Liu, J.-W., Xie, X., Zhang, Y., Lin, J., et al. (2014). Nitrification and its oxygen consumption along the turbid Chang Jiang River plume. *Biogeosciences*, *11*, 2083–2098. https://doi.org/10.5194/bg-11-2083-2014

Schouten, S., Hopmans, E. C., & Sinninghe Damsté, J. S. (2013). The organic geochemistry of glycerol dialkyl glycerol tetraether lipids: A review. *Organic Geochemistry*, *54*(0), 19–61. https://doi.org/10.1016/j.orggeochem.2012.09.006

Zhang, S. W., Wang, Q. Y., Lü, Y., Cui, H., & Yuan, Y. L. (2008). Observation of the seasonal evolution of the Yellow Sea Cold Water Mass in 1996–1998. *Continental Shelf Research*, *28*(3), 442–457. https://doi.org/10.1016/j.csr.2007.10.002

Zhang, Y., Xie, X., Jiao, N., Hsiao, S. S.-Y., & Kao, S.-J. (2014). Diversity and distribution of amoA-type nitrifying and nirS-type denitrifying microbial communities in the Yangtze River estuary. *Biogeosciences*, *11*(8), 2131–2145. https://doi.org/10.5194/bg-11-2131-2014